

Effect of heat treatment on microstructure, mechanical properties and in vitro degradation behavior of as-extruded Mg–2.7Nd–0.2Zn–0.4Zr alloy

ZHANG Xiao-bo, XUE Ya-jun, WANG Zhang-zhong

School of Materials Science and Engineering, Nanjing Institute of Technology, Nanjing 211167, China

Received 7 July 2012; accepted 30 August 2012

Abstract: Mg–2.7Nd–0.2Zn–0.4Zr (mass fraction, %) alloy was designed for degradable biomedical material. The ingots of the alloy were solution treated and then hot extruded. The extruded rods were heat treated with aging treatment, solution treatment and solution+aging treatment, respectively. Microstructures of the alloy were observed by optical microscopy (OM) and scanning electron microscopy (SEM). Mechanical properties at room temperature were tested. In vitro degradation behavior of the alloy immersed in simulated body fluid was measured by hydrogen evolution and mass loss tests. The degradation morphologies of the alloy with and without degradation products were observed by SEM. The results show that the grains grow apparently after solution treatment. Solution treatment improves the elongation of as-extruded alloy significantly and decreases the strength, while aging treatment improves the strength and reduces the elongation of the alloy. The yield ratio is reduced by heat treatment. The in vitro degradation results of the alloy show that solution treatment on the as-extruded alloy results in a little higher degradation rate and aging treatment on the alloy can reduce degradation rate slightly.

Key words: biodegradable magnesium alloy; mechanical properties; in vitro degradation behavior; heat treatment

1 Introduction

Biodegradable magnesium alloy is a new class of degradable biomaterials and they may be promising candidates for traditional biomedical alloys, such as Ti alloys and Co–Cr alloys, due to biodegradation, good biocompatibility, non-toxicity and other characteristics [1]. The most advanced clinical applications are biodegradable cardiovascular magnesium stents which have been successfully investigated in animals [2] and first clinical human trials have been conducted [3,4]. Magnesium alloys were also investigated as bone implants and can be applied in various designs, e.g. screws, plates or other fixture devices [5]. Previous researches on the feasibility of using biodegradable magnesium alloys for biomedical application mainly focused on the biocompatibility and corrosion resistance by coating [6–9]. But few studies [10] focused on how to improve strength of the biodegradable Mg alloys even though their strength is much lower than Ti alloys and Co–Cr alloys. In addition, as a biodegradable material,

the requirement for mechanical properties of magnesium alloy is different, e.g. high strength is needed for magnesium alloy used as bone implants, while high elongation is needed for magnesium alloy used as cardiovascular stents because the stent undergoes two plastic deformation during the implantation process.

Previous studies on biodegradable Mg–3.1Nd–0.2Zn–0.4Zr alloy indicate that lower extrusion temperature results in finer grains, higher strength and better corrosion resistance [11]. Lower extrusion ratio results in finer grains, higher strength and better corrosion resistance [12]. Furthermore, the alloy exhibits no cell toxicity [13] and shows better mechanical properties and corrosion resistance compared with commercial AZ31 and WE43 alloys [14]. In the present study, extrusion process was conducted on Mg–2.7Nd–0.2Zn–0.4Zr alloy with a low extrusion ratio at a relatively low temperature. The as-extruded alloy was then heat treated with different processes to adjust mechanical properties. Microstructure, mechanical properties at room temperature, in vitro degradation behavior in simulated body fluid were studied in order to

develop processes to control mechanical properties and degradation rate of biodegradable magnesium alloy for biomedical applications.

2 Experimental

Mg–2.7Nd–0.2Zn–0.4Zr alloy specimens cut from the cast ingots were solution-treated at 540 °C for 10 h and quenched into water at room temperature. The specimens were cut ($d 85 \text{ mm} \times 300 \text{ mm}$) by lathe to remove the oxidation surface and then hot extruded at 250 °C into rods ($d 30 \text{ mm}$, denoted as E) with an extrusion ratio of 8:1 and extrusion rate of 5 mm/s. Some extruded rods were aged at 200 °C for 8 h (denoted as EA). Some extruded rods were solution treated at 530 °C for 30 min (denoted as ES) and subsequently aged at 200 °C for 8 h (denoted as ESA).

The specimens for microstructure observation were cut parallel to extrusion direction, polished and then dried in warm flowing air. The polished specimens were etched with acid solution (20 mL acetic acid, 1 mL nitric acid, 60 mL glycol and 19 mL distilled water). The microstructures of the specimens were observed using an optical microscope (OM) and a scanning electron microscope (SEM) in back-scattered electron mode (BSE). Tensile test samples were cut parallel to the extrusion direction from respective rod. Tensile test was carried out on a material test machine at room temperature with a cross-head speed of 1 mm/min. Three specimens for each alloy were tested.

Hydrogen evolution and mass loss tests were conducted to evaluate in vitro degradation behavior of Mg alloy. Specimens for immersion tests with a dimension of 12 mm in diameter and 5 mm in thickness (total surface area: $(4.1 \pm 0.1) \text{ cm}^2$) were cut by an electric-sparking wire-cutting machine. The specimens were polished to mirror surface for immersion test. Simulated body fluid (SBF), which is composed of 8.0 g/L NaCl, 0.4 g/L KCl, 0.35 g/L NaHCO_3 , 0.2 g/L $\text{MgSO}_4 \cdot 7\text{H}_2\text{O}$, 0.14 g/L CaCl_2 , 0.06 g/L Na_2HPO_4 and 0.06 g/L KH_2PO_4 , was used as the test solution to study in vitro degradation behavior of the alloy. The pH value was adjusted to 7.4 with NaOH or HCl solution before experiments. Three specimens for each alloy were immersed in SBF at $(37 \pm 0.5) \text{ }^\circ\text{C}$ and the data were averaged. The ratio of surface area to solution volume is $1 \text{ cm}^2 : 30 \text{ mL}$ according to ASTM G31–72. The immersion test lasted for 240 h, and the SBF was renewed every 48 h in order to keep a relatively stable pH value of the solution and the hydrogen volume was recorded before renewing the SBF. The schematic illustration of the hydrogen evolution volume measurement can be referred to Ref. [15]. After the immersion test, the samples were removed from the

solution and cleaned in 200 g/L chromic acid solution with 10 g/L silver nitrate for 5 min to remove surface degradation products. The samples were rinsed with distilled water, ethanol, and then dried in warm flowing air. The dried samples were weighed and in vitro degradation rate was calculated. The morphologies of the immersion specimens were observed by SEM and the elements of the degradation products were analyzed by energy-dispersive spectrometry (EDS).

3 Results and discussion

3.1 Microstructure

Figure 1 shows the optical images of the alloy under various conditions. The microstructures of the E and EA consist of fine grains and long extrusion bands, as shown in Figs. 1(a) and (b). The fine grains of the E and EA, as the consequence of dynamic recrystallization, are so fine that can hardly be observed even under magnification of 1 000. According to the previous studies [12,16], long elongated grains formed along extrusion direction during hot extrusion, which have been suggested to arise from previous un-extruded structures that have survived dynamic recrystallization. Since these grains are favorably orientated to accommodate extrusion strains, in the basal slip system, they can undergo deformation without twinning and latent hardening. Hence, these grains do not have large enough stored plastic energy to trigger recrystallization. The long elongated grains locate in the extrusion bands even though they cannot be observed clearly by OM.

It is known that the precipitation can easily occur during hot extrusion and aging treatment for magnesium alloys, however, the precipitation phase cannot be observed clearly from Figs. 1(a), (b) and (d). After solution treatment on the as-extruded alloy, the grains become coarse apparently and the grain size of the coarse grains is over 40 μm , as shown in Fig. 1(c). Precipitation phase dissolves into Mg matrix after solution treatment. No obvious difference can be seen between the optical images of ES and ESA.

Figure 2 shows the SEM-BSE micrographs of the alloy. Bright phase can be observed in E and EA alloys, which precipitates during hot extrusion and is Mg_{12}Nd according to previous study [12]. The bright phase Mg_{12}Nd cannot be observed in ES alloy because it has been dissolved into matrix during solution treatment. No obvious difference of the alloy can be seen after aging treatment (E vs EA, ES vs ESA). In fact, the microstructure of the alloy after aging (EA and ESA) is composed of fine Nd-rich platelets in Mg matrix and these platelets are very small and cannot be seen in the optical images or even SEM images. The sizes of these plates are about 10 nm in diameter and 1–2 nm in thickness which can be observed by TEM [17].

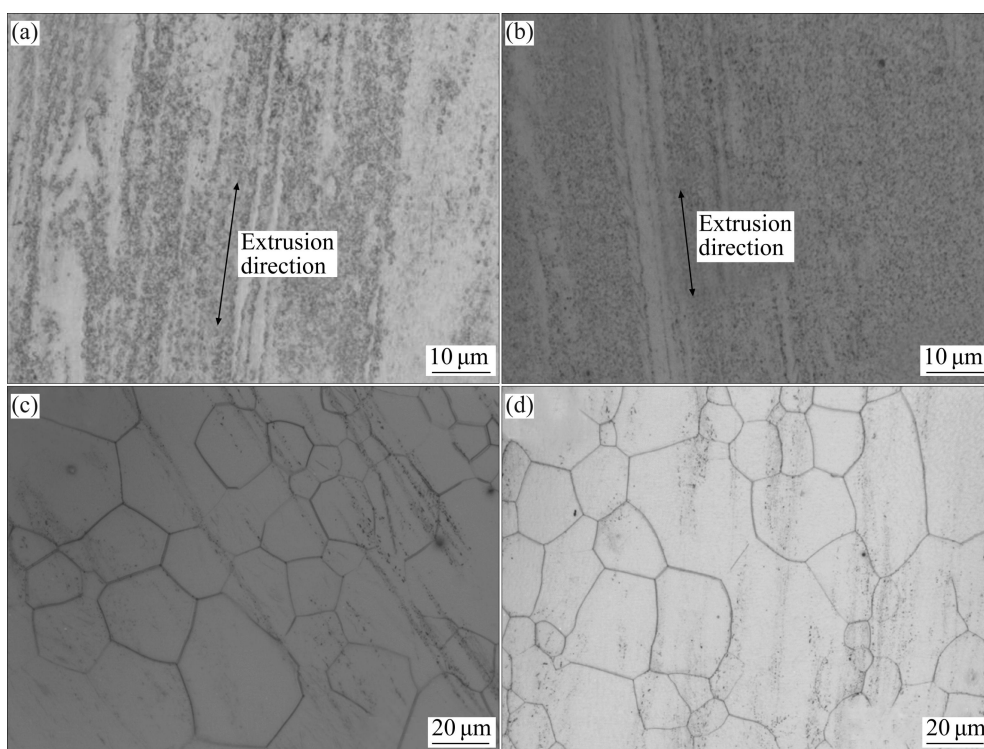


Fig. 1 Optical images of Mg-2.7Nd-0.2Zn-0.4Zr alloy: (a) E; (b) EA; (c) ES; (d) ESA

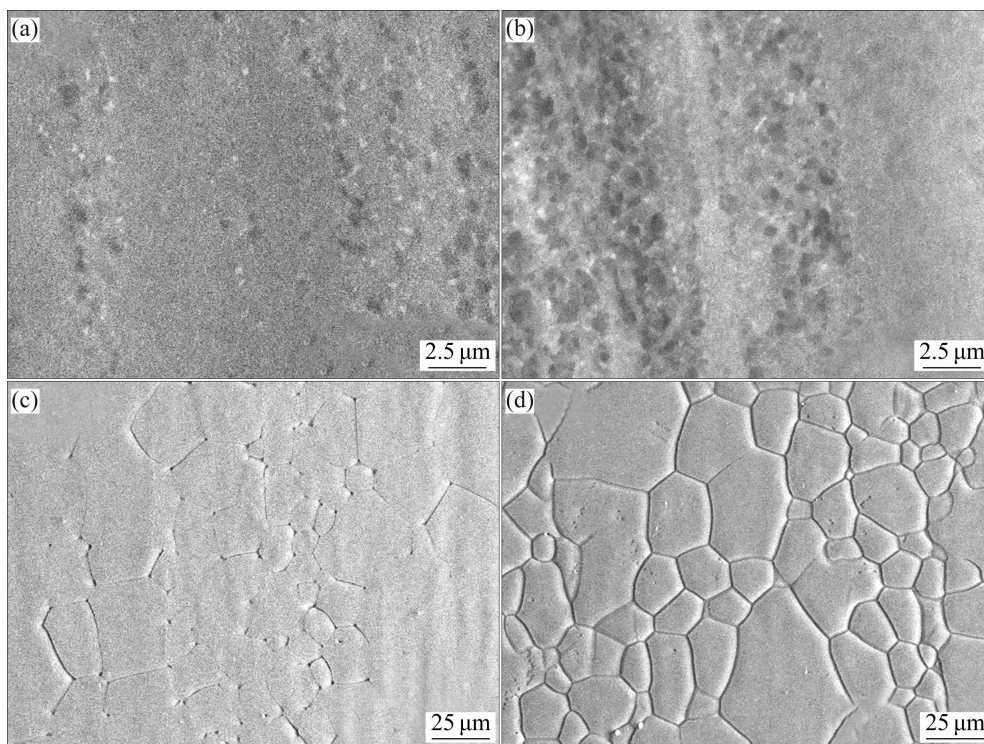


Fig. 2 SEM micrographs of Mg-2.7Nd-0.2Zn-0.4Zr alloy (a) E; (b) EA; (c) ES; (d) ESA

3.2 Mechanical properties

Mechanical properties of the Mg-2.7Nd-0.2Zn-0.4Zr alloy at room temperature are listed in Table 1. The yield strength ($\sigma_{0.2}$) and ultimate tensile strength (σ_b) of the as-extruded alloy (E) are both over 360 MPa and the elongation is about 8%. Both $\sigma_{0.2}$ and σ_b of the EA alloy

are improved up to about 400 MPa due to the precipitation strengthening caused by aging treatment while the elongation reduces. After solution treatment on the as-extruded alloy, $\sigma_{0.2}$ and σ_b drop obviously, however, the elongation is improved significantly. The grains become coarse after solution treatment, which results in

the decrease of the strength. Meanwhile, the microstructure is composed of equiaxed grains. The long elongated grains which are bad for elongation disappear, hence, the elongation improves significantly. Aging treatment on the ES alloy enhances the strength of ES alloy greatly due to precipitation strengthening but the elongation decreases.

Table 1 Mechanical properties of Mg-2.7Nd-0.2Zn-0.4Zr alloy tested at room temperature

Specimen	$\sigma_{0.2}$ /MPa	σ_b /MPa	$\sigma_{0.2}/\sigma_b$	δ /%
E	363±6.3	376±4.3	0.96	8.4±2.2
EA	394±5.2	417±7.6	0.94	2.6±0.2
ES	121±4.8	217±3.3	0.56	22.2±2.4
ESA	191±2.6	326±2.8	0.59	12.2±1.2

Additionally, the yield ratios ($\sigma_{0.2}/\sigma_b$) of the E and EA are very high, which indicates that the value of $\sigma_{0.2}$ is close to that of σ_b . However, the yield ratios of the ES and ESA are moderate. A basal slip system can be easily activated and then accelerates the accumulation of dislocation during plastic deformation, which is the origin of work hardening. However, the highest dislocation density of the as-extruded alloy almost reaches the critical level, which restricts further dislocation accumulation and work hardening [18]. However, after solution treatment, the larger grain size and the lower dislocation density in grains are beneficial to the dislocation accumulation which generates work hardening during tensile deformation. Therefore, remarkable work hardening occurs in the solution treated alloy. The yield ratio of the alloy can be adjusted effectively between 0.98 and 0.55 by controlling heat treatment parameters, which is not reported here. The magnesium alloys with high strength (E and EA) will be a promising candidates to be applied as bone implants and those with low yield ratio and good elongation (ES and ESA) will be a promising candidates to be applied as cardiovascular stents.

3.3 In vitro degradation behavior

Figure 3 shows the hydrogen evolution volume of the Mg-2.7Nd-0.2Zn-0.4Zr alloy immersed in SBF for 240 h. It can be seen that the hydrogen evolution volume of the alloy under different conditions shows only slight difference which even cannot be distinguished. The total hydrogen evolution of the E, EA, ES and ESA after 240 h immersion is 1.34, 1.28, 1.47 and 1.38 mL/cm², respectively. The result shows that solution treatment plays a slight negative role while aging treatment plays a slight positive role on in vitro degradation behavior of the alloy. Moreover, the hydrogen volume of the alloy

under different conditions shows a decrease trend with the increase of immersion time. The hydrogen evolution during the first 48 h is much more than that during subsequent immersion time. It is possible that the corrosion layer on the surface of the alloy becomes thick, which can prevent matrix from exposing in SBF and thus stifled degradation.

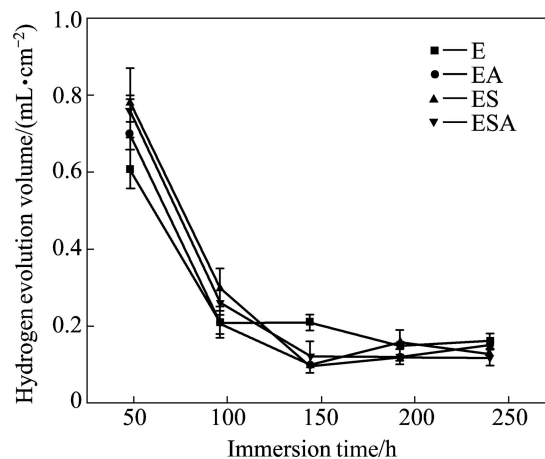


Fig. 3 Hydrogen evolution volume of Mg-2.7Nd-0.2Zn-0.4Zr alloy immersed in SBF for 240 h

Figure 4 shows the mass loss test results of the alloy immersed in SBF for 240 h. It reveals that the in vitro degradation rate of E is a little slower than that of ES, which indicates that solution treatment plays a slight negative role on degradation rate. The degradation rate of EA is a little slower than that of E, and the degradation rate of ES is a little lower than that of ESA, which suggests that aging treatment can reduce the degradation rate slightly. The result of mass loss test has a good agreement with that of the hydrogen evolution test.

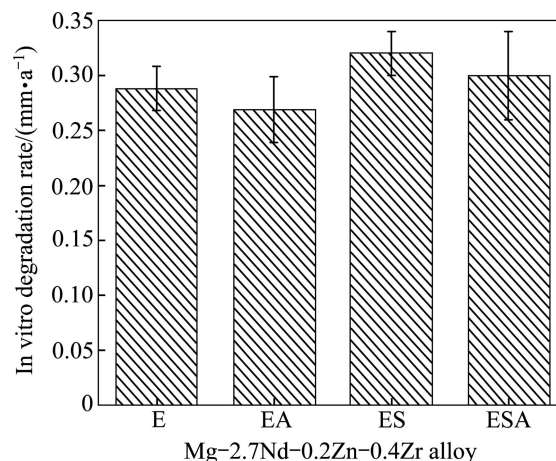


Fig. 4 In vitro degradation rate of Mg-2.7Nd-0.2Zn-0.4Zr alloy immersed in SBF for 240 h

Figure 5 shows the degradation product morphologies of the alloy after immersion in SBF for

240 h. It can be observed that the degradation products are composed of two parts, which are compact film on the surface of the matrix and white particles on the film. The compact film formed on the surface of the matrix may play a protect role on degradation. Therefore, the hydrogen evolution volume of the alloy shows decreasing trend with lasting immersion time. In addition,

the film on the surface of the matrix is separated by lots of visible cracks. The cracks are actually caused by drying the specimen after immersion test. EDS test is conducted on E in order to identify the degradation products of the alloy. The results shown in Fig. 6 indicate that the white particles on the film contain O, Ca, P and Mg elements and the compact film contains O, Mg, P

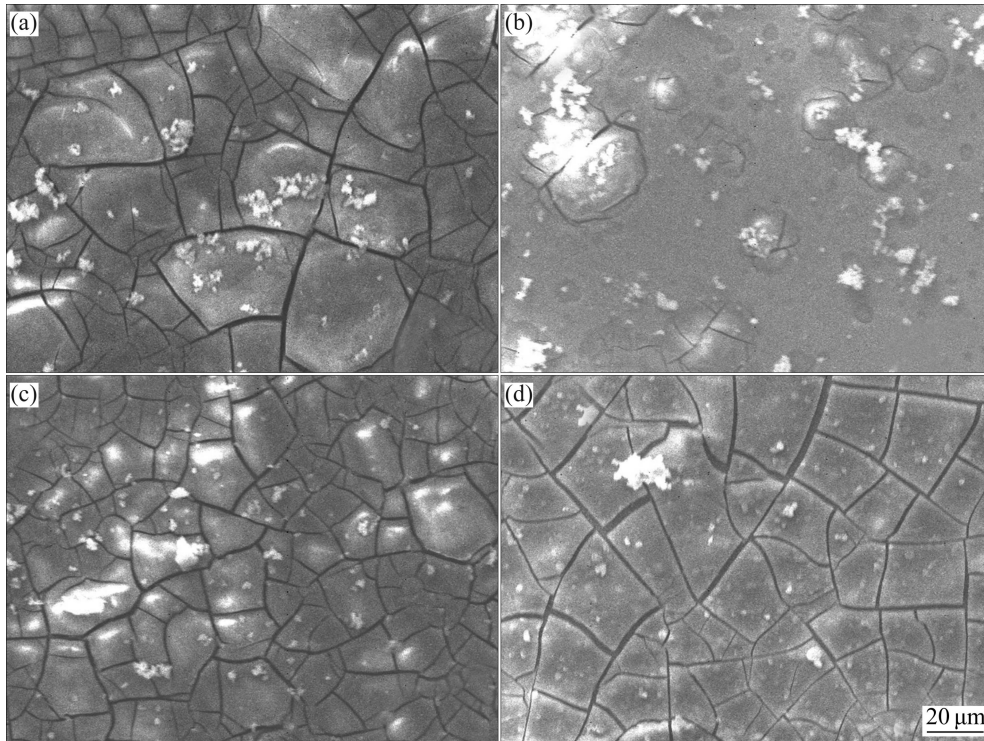


Fig. 5 SEM images showing degradation product morphologies of Mg-2.7Nd-0.2Zn-0.4Zr alloy immersed in SBF for 240 h: (a) E; (b) EA; (c) ES; (d) ESA

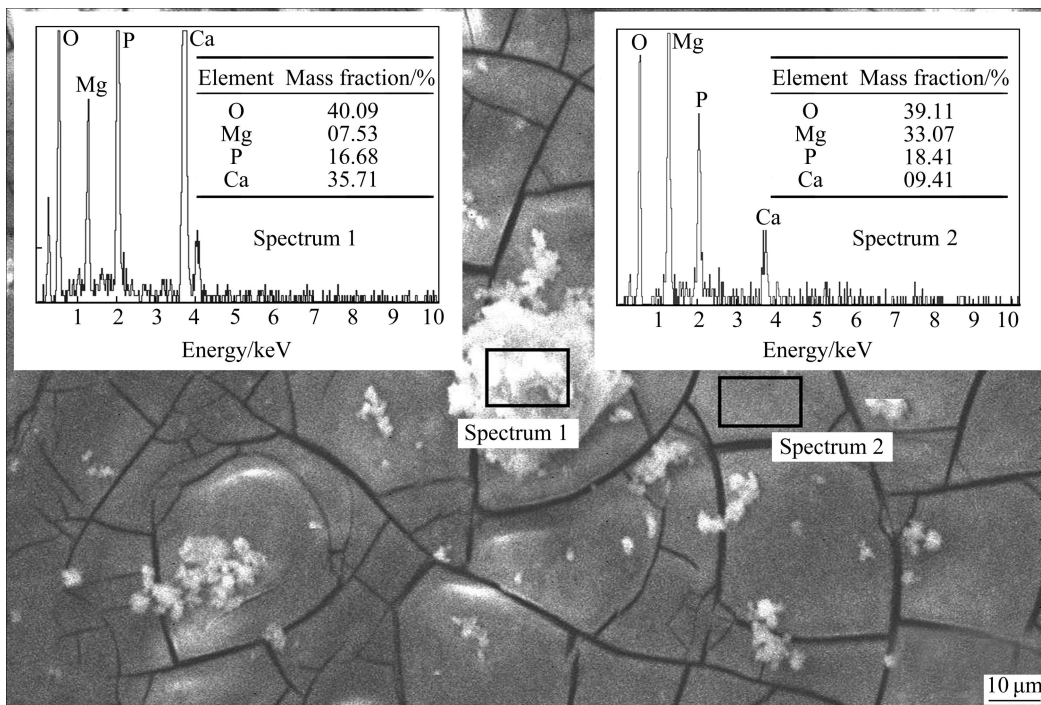


Fig. 6 EDS results of degradation products of E after immersion in SBF for 240 h

and Ca. According to the previous study [11], the compact film on the surface of matrix is mainly $\text{Mg}(\text{OH})_2$ with some Ca and P, and the white particles are mainly $\text{Ca}_{10}(\text{PO}_4)_6(\text{OH})_2$ and $\text{Mg}(\text{OH})_2$. The formation of $\text{Ca}_{10}(\text{PO}_4)_6(\text{OH})_2$ particles on the Mg substrate surface can accelerate the bone tissue to heal, which indicates that the Mg alloy has good biocompatibility.

Figure 7 shows the degradation morphologies of the alloy after removing degradation products. Numerous tiny pits are visible on the surface of the alloy and some large pits can be seen in ES. In general, the degradation morphologies of the alloy are uniform, which is different from localized corrosion with large holes on the surface of matrix, such as Mg–Zn alloy [19]. Uniform degradation is important for biodegradable materials. Localized degradation probably causes a collapse of the implant even though the degradation rate of the implant is slow. Contrarily, the whole collapse of the implant caused by localized degradation can be avoided if the implant exhibits a uniform degradation mode.

Both hydrogen evolution and mass loss results show that solution treatment on the as-extruded alloy increases degradation rate slightly while aging treatment on both as-extruded and solution treated alloy decreases degradation rate slightly. The results may be due to the grain size, precipitation phase and internal stress of the alloy. It was reported that fine grains could enhance the

corrosion resistance of magnesium alloy [20–22]. However, the second phase Mg_{12}Nd is precipitated during hot extrusion in E alloy, which can induce galvanic corrosion. The second phase is dissolved into matrix during solution treatment, and thus the factor by galvanic corrosion is eliminated. Therefore, the better corrosion resistance of the E than ES is attributed to finer grains. As for the influence of aging treatment on degradation behavior of the alloy, it is mentioned that precipitation phase with nano size is formed during aging, which can also cause microgalvanic corrosion. Nevertheless, internal stress in E and ES alloys caused by hot extrusion and quenching, respectively, should play a negative role on corrosion resistance [23]. The internal stress can be relieved by aging. Consequently, the improved corrosion resistance of the alloy caused by aging treatment is mainly ascribed to the relief of internal stress.

4 Conclusions

1) Precipitation phase of Mg–2.7Nd–0.2Zn–0.4Zr alloy caused by hot extrusion can be dissolved into matrix by solution treatment, but the grains become coarse simultaneously. No obvious difference in the microstructures before and after aging treatment can be observed by OM or SEM.

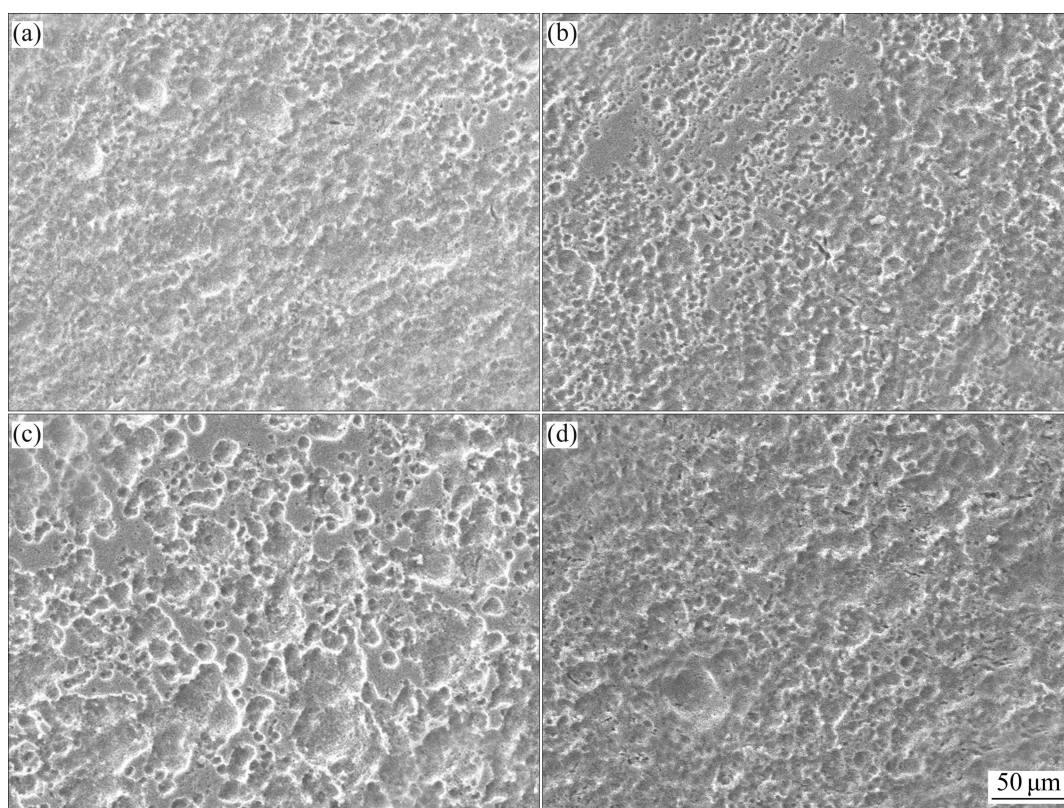


Fig. 7 SEM images showing morphologies of Mg–2.7Nd–0.2Zn–0.4Zr alloy immersed in SBF for 240 h after removing degradation products: (a) E; (b) EA; (c) ES; (d) ESA

2) Solution treatment on the as-extruded Mg–2.7Nd–0.2Zn–0.4Zr alloy can reduce yield ratio and improve the elongation of alloy significantly, while aging treatment on the solution treated alloy can enhance strength apparently due to the precipitation strengthening.

3) Due to the coarse microstructure, in vitro degradation rate of the alloy increases slightly by solution treatment. Even though the precipitation phase is formed, which is bad for corrosion resistance, because of the relief of internal stress, the degradation rate of the alloy is reduced by aging treatment.

Acknowledgment

The authors would like to appreciate Professor YUAN Guang-yin at Shanghai Jiao Tong University for his great contribution to this work.

References

- [1] SONG Y W, SHAN D Y, CHEN R S, ZHANG F, HAN E H. Biodegradable behaviors of AZ31 magnesium alloy in simulated body fluid [J]. *Materials Science and Engineering C*, 2009, 29(3): 1039–1045.
- [2] HEUBLEIN B, ROHDE R, KAESE V, NIEMEYER M, HARTUNG W, HAVERICH A. Biocorrosion of magnesium alloys: A new principle in cardiovascular implant technology [J]. *Heart*, 2003, 89(6): 651–656.
- [3] ZARTNER P, CESNJEVAR R, SINGER H, WEYAND M. First successful implantation of a biodegradable metal stent into the left pulmonary artery of a preterm baby [J]. *Catheterization and Cardiovascular Interventions*, 2005, 66 (4): 590–594.
- [4] ERBEL R, MARIO C D, BARTUNEK J, BONNIER J, BRUYNE B, EBERLI F R, ERNE P, HAUDE M. Temporary scaffolding of coronary arteries with bioabsorbable magnesium stents: A prospective, non-randomised multicentre trial [J]. *Lancet*, 2007, 369(9576): 1869–1875.
- [5] WITTE F, HORT N, VOGT C, COHEN S, KAINER K U, WILLUMEIT R, FEYERABEND F. Degradable biomaterials based on magnesium corrosion [J]. *Current Opinion in Solid State and Materials Science*, 2008, 12(5/6): 63–72.
- [6] GU X N, LI N, ZHOU W R, ZHENG Y F, ZHAO X, CAI Q Z, RUAN L Q. Corrosion resistance and surface biocompatibility of a microarc oxidation coating on a Mg–Ca alloy [J]. *Acta Biomaterialia*, 2011, 7(4): 1880–1889.
- [7] LI J N, CAO P, ZHANG X N, ZHANG S X, HE Y H. In vitro degradation and cell attachment of a PLGA coated biodegradable Mg–6Zn based alloy [J]. *Journal of Materials Science*, 2010, 45(22): 6038–6045.
- [8] GU X N, ZHENG Y F, CHENG Y, ZHONG S P, XI T F. In vitro corrosion and biocompatibility of binary magnesium alloys [J]. *Biomaterials*, 2009, 30(4): 484–498.
- [9] ZHANG C Y, ZENG R C, CHEN R S, LIU C L, GAO J C. Preparation of calcium phosphate coatings on Mg–1.0Ca alloy [J]. *Transactions of Nonferrous Metals Society of China*, 2010, 20(s2): s655–s659.
- [10] HE S Y, SUN Y, CHEN M F, LIU D B, YE X Y. Microstructure and properties of biodegradable β -TCP reinforced Mg–Zn–Zr composites [J]. *Transactions of Nonferrous Metals Society of China*, 2011, 21(4): 814–819.
- [11] ZHANG X B, YUAN G Y, MAO L, NIU J L, FU P H, DING W J. Effects of extrusion and heat treatment on the mechanical properties and bio-corrosion behaviors of a Mg–Nd–Zn–Zr alloy [J]. *Journal of the Mechanical Behavior of Biomedical Materials*, 2012, 7: 77–86.
- [12] ZHANG X B, YUAN G Y, MAO L, NIU J L, FU P H, DING W J. Microstructure, mechanical properties and in vitro degradation behaviors of as-extruded Mg–Nd–Zn–Zr alloy with different extrusion ratios [J]. *Journal of the Mechanical Behavior of Biomedical Materials*. 2012, 9: 153–162.
- [13] YUAN Guang-yin, ZHANG Xiao-bo, NIU Jia-lin, TAO Hai-rong, CHEN Dao-yun, HE Yao-hua, JIANG Yao, DING Wen-jiang. Research progress of new type of degradable biomedical magnesium alloys JDBM [J]. *The Chinese Journal of Nonferrous Metals*, 2011, 21(10): 2476–2488. (in Chinese)
- [14] ZHANG X B, YUAN G Y, MAO L, NIU J L, DING W J. Biocorrosion properties of as-extruded Mg–Nd–Zn–Zr alloy compared with commercial AZ31 and WE43 alloys [J]. *Materials Letters*, 2012, 66(1): 209–211.
- [15] ZONG Y, YUAN G Y, ZHANG X B, MAO L, NIU J L, DING W J. Comparison of biodegradable behaviours of AZ31 and Mg–Nd–Zn–Zr alloys in Hank's physiological solution [J]. *Materials Science and Engineering B*, 2012, 177(5): 395–401.
- [16] ZHANG X B, YUAN G Y, WANG Z Z. Mechanical properties and biocorrosion resistance of Mg–Nd–Zn–Zr alloy improved by cyclic extrusion and compression [J]. *Materials Letters*, 2012, 74: 128–131.
- [17] FU P H, PENG L M, JIANG H Y, CHANG J W, ZHAI C Q. Effects of heat treatments on the microstructures and mechanical properties of Mg–3Nd–0.2Zn–0.4Zr (wt.%) alloy [J]. *Materials Science and Engineering A*, 2008, 486(1/2): 183–192.
- [18] ZHANG B P, GENG L, HUANG L J, ZHANG X X, DONG C C. Enhanced mechanical properties in fine-grained Mg–1.0Zn–0.5Ca alloys prepared by extrusion at different temperatures [J]. *Scripta Materialia*, 2010, 63(10): 1024–1027.
- [19] ZHANG S X, ZHANG X N, ZHAO C L, LI J N, SONG Y, XIE C Y, TAO H R, ZHANG Y, HE Y H, JIANG Y, BIAN Y J. Research on an Mg–Zn alloys as a biodegradable biomaterial [J]. *Acta Biomaterialia*, 2010, 6(2): 626–640.
- [20] LIU C L, XIN Y C, TANG G Y, CHU PK C.L. Influence of heat treatment on degradation behavior of bio-degradable die-cast AZ63 magnesium alloy in simulated body fluid [J]. *Materials Science and Engineering A*, 2007, 456(1/2): 350–357.
- [21] HAMU G B, ELIEZER D, WAGNER L. The relation between severe plastic deformation microstructure and corrosion behavior of AZ31 magnesium alloy [J]. *Journal of Alloys and Compounds*, 2009, 468(1/2): 222–229.
- [22] ALVAREZ-LOPEZ M, PEREDA M D, VALLE J A, FERNANDEZ-LORENZO M, GARCIA-ALONSO M C, RUANO O A, ESCUDERO M L. Corrosion behaviour of AZ31 magnesium alloy with different grain sizes in simulated biological fluids [J]. *Acta Biomaterialia*, 2010, 6(5): 1763–1771.
- [23] WINZER N, ATRENS A, DIETZEL W, SONG G, KAINER K U. Magnesium stress corrosion cracking [J]. *Transactions of Nonferrous Metals Society of China*, 2007, 17(s1): s150–s155.

热处理对挤压态 Mg-2.7Nd-0.2Zn-0.4Zr 合金组织、力学性能和体外降解行为的影响

章晓波, 薛亚军, 王章忠

南京工程学院 材料科学与工程学院, 南京 211167

摘要: 设计了 Mg-2.7Nd-0.2Zn-0.4Zr(质量分数, %)镁合金作为可降解生物医用材料。对固溶处理后的铸锭进行了热挤压处理, 然后对挤压棒分别进行了时效处理、固溶处理及固溶+时效处理。利用光学显微镜和扫描电镜观察了合金的组织, 测试了合金的室温力学性能, 采用析氢和失重法测试了合金在模拟体液中的降解行为, 用扫描电镜观察了降解产物形貌及洗去降解产物后的形貌。结果表明: 固溶处理后合金的晶粒明显长大, 固溶处理显著提高挤压态合金的伸长率, 但降低了合金的强度, 而时效处理可提高合金的强度, 降低合金的伸长率; 热处理可降低合金的屈强比。体外降解实验结果表明: 固溶处理使合金的降解速率稍微加快, 而时效处理则能稍微减慢合金的降解速率。

关键词: 生物可降解镁合金; 力学性能; 体外降解行为; 热处理

(Edited by LI Yan-hong)